

# Comparative study of strategies for creep simulation in the calculation of second-order effects in reinforced concrete columns

Lucas S. P. Teixeira<sup>1</sup>, Leandro L. Silva<sup>1</sup>, Juliano S. Becho<sup>1</sup>

<sup>1</sup>*Dept. of Structural Engineering, Federal University of Minas Gerais  
Antônio Carlos Avenue, 6627, 31270-901, Belo Horizonte/Minas Gerais, Brazil  
lucasspt@ufmg.br; leandro@dees.ufmg.br; julianobecho@dees.ufmg.br*

**Abstract.** This study investigates the effects of creep in reinforced concrete columns using various strategies. Creep is the phenomenon of increasing deformations in concrete over time under constant stress. This topic is especially relevant in reinforced concrete columns, where creep can cause increased forces as well as increased second-order moments. The complexity of the creep phenomenon has led to the dominance of simplified methods. This work conducts a comparative analysis of commonly used methods for simulating creep. The strategies considered are the Approximate Method of Additional Eccentricity  $e_{cc}$  and the Standard-Column Method coupled with M, N,  $1/r$  Diagrams considering creep effects through extended stress-strain curve. An implementation in the Java programming language is used to obtain the results for the different analyzed methods. A case study of a simply supported column was simulated to compare the results. The present study concludes that the Additional Eccentricity Method yields higher moment values, whereas the Standard-Column Method coupled with M, N,  $1/r$  Diagrams generates results close to more refined models.

**Keywords:** Creep, Reinforced concrete columns, Second-order analysis

## 1 Introduction

The structural analysis of reinforced concrete columns is particularly complex. According to Casagrande [1], due to their predominantly vertical structure, these components are susceptible to instability that result in significant geometric nonlinearity, in addition to physical nonlinearity inherent to the use of reinforced concrete. Additionally, it is important to consider rheology, with emphasis on the effect of creep, which can cause an increase in internal forces as well as an increase in second-order moments.

Creep is defined as the phenomenon of increasing deformations in concrete over time when subjected to constant stress. This behavior results from the viscoelastic properties of the material. As pointed out by Ballim and Fanourakis [2], concrete creep can be beneficial by providing the concrete with a necessary degree of ductility. On the other hand, this slow deformation often results in excessive deflections in service conditions, potentially leading to structural instability, crack formation, and significant loss of straightness in tall columns.

The simulation of creep can become challenging due to the dependence of this phenomenon on various factors, such as ambient humidity and temperature, the age and cracking of the concrete, loading duration, and the dimensions of structural elements [3]. In the literature, several constitutive models are not widely used due to their complexity, with simplified methods being dominant in design practice.

This work is a comparative study of simplified methods for considering creep in reinforced concrete columns. In this study, the Approximate Method of Additional Eccentricity  $e_{cc}$  and the Standard-Column Method coupled with M, N,  $1/r$  Diagrams considering creep effects through extended stress-strain curve.

## 2 Second-order effects in reinforced concrete columns

Carvalho and Pinheiro [4] define second-order effects as those that are added to the results obtained from a first-order analysis - where the structure is analyzed in its initial geometric configuration - when the equilibrium analysis of the structure is performed in its deformed configuration.

ABNT NBR 6118 [5] defines, according to the slenderness ratio  $\lambda$  of the column, appropriate methods for calculating second-order effects. The slenderness ratio expresses the relation between the cross-sectional dimensions

and the height of the element, considering its boundary conditions [1]. This parameter is determined by

$$\lambda = \frac{\ell_e}{i} \quad (1)$$

where  $\ell_e$  is the effective length of the column and  $i$  represents the radius of gyration.

## 2.1 Standard-Column Method

As explained by Carvalho and Pinheiro [4], the approximate methods based on the standard-column seek to identify the most stressed section of the column and, through simplifications, establish expressions for calculating second-order effects. This method is applicable to columns with a constant cross-section, including their reinforcement, along their entire length [6].

According to Fusco [6], the standard-column is a cantilever column with an effective length  $\ell_e = 2l$ , as illustrated in Fig. 1. The method assumes a curvature distribution that generates a deflection  $a$  at the free end of the column given by

$$a = \frac{\ell_e^2}{10} \left( \frac{1}{r} \right) \quad (2)$$

where  $1/r$  is the curvature of the section with the maximum deflection and  $\ell_e$  is the effective length of the column.

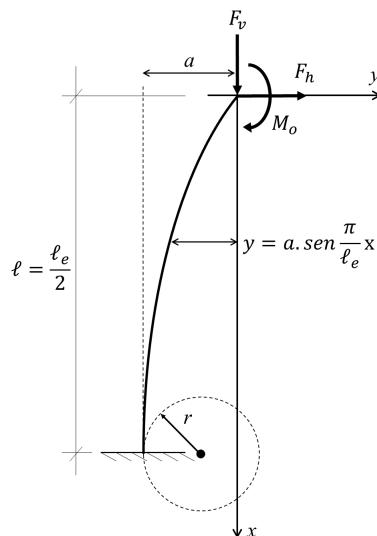


Figure 1. Standard-Column. Adapted from Fusco [6].

In the standard-column, the maximum deflection is a linear function of the curvature of the bar, as shown in eq. (2). The curvature is approximately expressed by the second derivative of the elastic line equation, which is assumed to be a sine function [4]. Thus, the grounding of this method is demonstrated, starting from the consideration that the elastic line of the bar axis is given by

$$y(x) = -a \sin\left(\frac{\pi}{\ell_e} x\right). \quad (3)$$

Assuming a small displacement regime, the curvature ( $1/r$ ) can be expressed as the second derivative of the elastic line, resulting in

$$\frac{1}{r} = \frac{d^2 y}{dx^2} = a \left(\frac{\pi}{\ell_e}\right)^2 \sin\left(\frac{\pi}{\ell_e} x\right). \quad (4)$$

By setting  $x = \ell_e/2$  for the base section and approximating  $\pi^2 \cong 10$ , we obtain eq. (2). In this method, the second-order eccentricity ( $e_2$ ) is assumed to be equal to the deflection  $a$  and can be written as

$$e_2 = \frac{\ell_e^2}{10} \left( \frac{1}{r} \right). \quad (5)$$

In this work, the Standard-Column Method is applied coupled with M, N,  $1/r$  diagrams. According to ABNT NBR 6118 [5] this method can be applied to columns with  $\lambda \leq 140$ . The physical non-linearity is considered by determining the curvature of the critical section from specific M, N,  $1/r$  diagrams.

The total maximum moment within the column  $M_{d,tot}$  is calculated as a function of the dimensionless stiffness  $\kappa$  by

$$M_{d,tot} = \frac{\alpha_b M_{1d,A}}{1 - \frac{\lambda^2}{120\kappa/\nu}} \geq M_{1d,A} \quad (6)$$

where  $M_{1d,A}$  is the design value of the first-order moment  $M_A$ , the parameter  $\alpha_b$  depends on the boundary conditions at the column ends and the shape of the first-order moment diagram, and  $\nu$  is the dimensionless axial force. In the Standard-Column Method coupled with M, N,  $1/r$ , the stiffness  $\kappa$  is taken as the secant stiffness  $\kappa_{sec}$ , obtained by

$$\kappa_{sec} = \frac{(EI)_{sec}}{A_c h^2 f_{cd}} \quad (7)$$

where  $(EI)_{sec}$  represents the slope of the secant line of the M, N,  $1/r$  diagram (Fig. 2).

## 2.2 M, N, $1/r$ diagram

ABNT NBR 6118 [5] states that the effect of physical non-linearity can be considered through the construction of a material relationship known as the moment-axial force-curvature (M, N,  $1/r$ ) diagram. This relation represents the response of the reinforced concrete cross-section under the combined action of a constant axial force and a progressively increasing bending moment, obtained by considering the actual strains of concrete and steel [1]. This diagram must be constructed for each section with known reinforcement and for the value of the acting axial force.

ABNT NBR 6118 [5] also proposes the consideration of a “safety formulation”, in which the material M, N,  $1/r$  diagram is constructed by considering the forces previously increased by  $\gamma_f/\gamma_{f3}$ , and the results of the analysis are subsequently increased by only the remaining coefficient  $\gamma_f$ , i.e.,  $\gamma_{f3}$ , which has a value of 1.1. Additionally, the deformability of the elements should be calculated based on the idealized stress-strain curves for concrete and steel, with the peak stress of concrete taken as  $1.10f_{cd}$ . The graphical representation of the moment-curvature relationship is illustrated in Fig. 2.

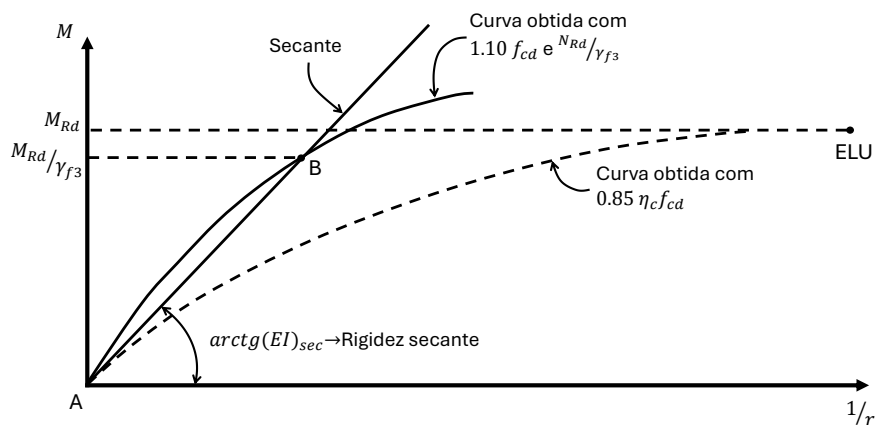


Figure 2. Moment-curvature diagram. Adapted from ABNT NBR 6118 [5].

The dashed curve, obtained with the design values of the strengths of concrete and steel, is used to determine the resistant moment  $M_{Rd}$  corresponding to the axial force  $N_{Rd}$  (maximum point), aiming to determine point B. For the purpose of using the Standard-Column Method coupled with M, N,  $1/r$  Diagrams, the curve AB can be linearized, for safety reasons by the line AB, characterizing the secant stiffness  $(EI)_{sec}$ .

### 3 Creep simulation

This section presents the simplified strategies for creep simulation used in this work. These strategies can be utilized in conjunction with the Standard-Column Method. The strategies employed in this work are based on the creep coefficient  $\varphi$ , which allows for the characterization of the creep phenomenon using a single parameter, independent of the applied stress. This parameter can be calculated in a simplified manner by linear interpolation from Table 8.1 of ABNT NBR 6118 [5] or by the rigorous calculation procedure described in Appendix A of this Standard.

The deformation  $\varepsilon_{cc}$  caused by creep is calculated by multiplying the immediate concrete deformation  $\varepsilon_c$  by  $\varphi$

$$\varepsilon_{cc} = \varphi \varepsilon_c. \quad (8)$$

The total deformation  $\varepsilon_{c,total}$  can be calculated as

$$\varepsilon_{c,total} = \varepsilon_c + \varepsilon_{cc} = (1 + \varphi)\varepsilon_c. \quad (9)$$

#### 3.1 Approximate Method of Additional Eccentricity $e_{cc}$

In the simulation of local second-order effects in columns, ABNT NBR 6118 [5] allows for the approximate consideration of creep through the additional eccentricity  $e_{cc}$ , calculated as

$$e_{cc} = \left( \frac{M_{sg}}{N_{sg}} + e_a \right) \left( 2.718^{\frac{\varphi N_{sg}}{N_e - N_{sg}}} - 1 \right) \quad (10)$$

where

- $N_e = \frac{10E_{ci}I_c}{\ell_e^2}$  is the Euler critical load;
- $e_a$  is the eccentricity due to local imperfections, calculated according to ABNT NBR 6118 [5];
- $M_{sg}$  and  $N_{sg}$  are the applied moments and axial forces due to the quasi-permanent combination;
- $\varphi$  is the creep coefficient;
- $E_{ci}$  is the initial tangent modulus of elasticity of concrete;
- $I_c$  is the moment of inertia of the concrete section;
- $\ell_e$  is the buckling length of the column.

The additional eccentricity  $e_{cc}$  must be considered in the total eccentricity, as if it were an immediate effect that adds to the initial eccentricity  $e_1$ .

#### 3.2 Standard-Column Method coupled with M, N, 1/r Diagrams with incorporated creep

In the use of the Standard-Column Method coupled with M, N, 1/r Diagrams, creep can be incorporated through the use of the extended stress-strain curve for the construction of the M, N, 1/r diagrams.

The construction of the extended stress-strain curve is based on the principle that the creep strain  $\varepsilon_{cc}$  is calculated by multiplying the immediate concrete strain  $\varepsilon_c$  by  $\varphi$  according to eq. (9).

Thus, the stress-strain diagram undergoes a parallel shift along the  $\varepsilon_c$  axis by a factor of  $\varphi$ , as shown in Fig. 3.

In the application of this method, Westerberg [7] suggests using  $\varphi_{ef}$  to account for the difference in the influence of short-term and long-term loads on the creep phenomenon. This method is included in the EN 1992-1-1 [8], although it is not present in ABNT NBR 6118 [5].

By applying these concepts, it is possible to obtain the M, N, 1/r diagram considering creep

$$\left( \frac{1}{r} \right)_{total} = \frac{\varepsilon_s + \varepsilon_{c,total}}{d} \therefore \left( \frac{1}{r} \right)_{total} = \frac{\varepsilon_s + (1 + \varphi)\varepsilon_c}{d} \quad (11)$$

where  $d$  is the effective depth of the section, i.e., the distance between the centroid of the area of tension reinforcement and the most compressed fiber of the section.

After obtaining the M, N, 1/r diagram with incorporated creep, it is possible to apply the Standard-Column Method, as presented in section 2.1, obtaining a secant stiffness  $\kappa_{sec}$  according to eq. (7).

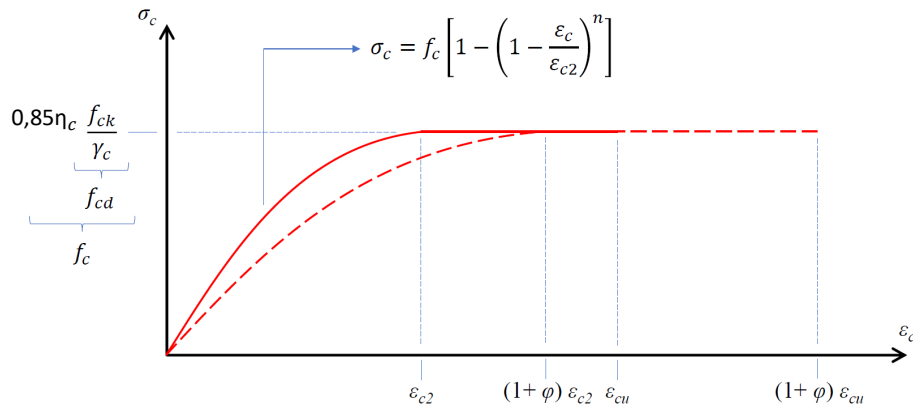


Figure 3. Extended stress-strain curve due to the consideration of creep.

## 4 Methodology

For the application of the described methods, an algorithm was developed in the Java programming language. This implementation is particularly necessary for constructing M, N,  $1/r$  diagrams, which is a complex process involving iterative calculations and successive approximations [1].

The algorithm was developed to construct the moment-curvature diagrams for a column under combined axial force and bending moment with a fixed axial force value, N, based on the formulation presented by de Paula [9]. Besides the fixed axial force, the program requires the input of the cross-sectional characteristics, including its geometric properties, material parameters of the concrete and steel, and the area and position of the reinforcement.

The program starts constructing the diagram with an initial curvature close to zero. In each iteration, the lower and upper limits for the neutral axis depth variation are defined, ensuring that the section response does not exceed the ultimate strains of steel and concrete. From this range of values, the False Position Method is used to find the neutral axis depth that balances the section with the fixed axial force. If equilibrium is not possible, this point is discarded. Otherwise, the resistant bending moment value is calculated for the found neutral axis depth, and this point is recorded in the diagram. Finally, an increment is applied to the initial curvature, initiating a new iteration.

The construction of the diagram is performed twice. The first one is done for the ultimate strength in the concrete  $\sigma_{cd}$  equal to  $0.85\eta_c f_{cd}$  to obtain the resistant moment  $M_{Rd}$  corresponding to the normal force  $N_{Rd}$ , which corresponds to the configuration where the strains in the steel or concrete reach their limit values (dashed curve in Fig. 2) [1]. The second curve is constructed for  $\sigma_{cd} = 1.1f_{cd}$  to obtain the point B in Fig. 2. From this point, the secant stiffness  $(EI)_{sec}$  corresponding to the slope of line AB is obtained and its dimensionless representation  $\kappa_{sec}$ .

The program also allows the construction of the M, N,  $1/r$  diagram with incorporated creep by introducing the creep coefficient  $\varphi$  in the construction of the stress-strain curve, which generates an extended curve, as shown in Fig. 3.

The algorithm for the Standard-Column Method and the Approximate Method of Additional Eccentricity  $e_{cc}$  are relatively simple and essentially consist of implementing the equations presented for each method. For the Standard-Column Method, the constructed M, N,  $1/r$  diagram is used as an input parameter, to apply the dimensionless secant stiffness  $\kappa_{sec}$ .

## 5 Practical application and results

As a case study to compare the results obtained for the different methods presented, an example taken from Casagrande [1] was implemented.

It is a simply supported column with a rectangular cross-section, an equivalent length  $\ell_e = 3.0$  m and subjected to a design load  $N_{Sd} = 2100$  kN, as shown in the schematic drawing in Fig. 4a. In addition to the axial force, the column is also subjected to a first-order bending moment diagram as illustrated in Fig. 4b. The concrete is class C30 (characteristic compressive strength of concrete  $f_{ck} = 30$  MPa) and the steel is CA-50 (characteristic yield strength  $f_{yk} = 500$  MPa). A creep coefficient  $\varphi = 2.0$  is adopted.

Starting with the application of the Standard-Column Method without considering creep, the M, N,  $1/r$  diagrams are obtained as shown in Fig. 5. In the same figure, the diagrams obtained for the design values and for

the safety formulation, in the developed program and in the work of Casagrande [1] are represented. The figure shows that both results converged.

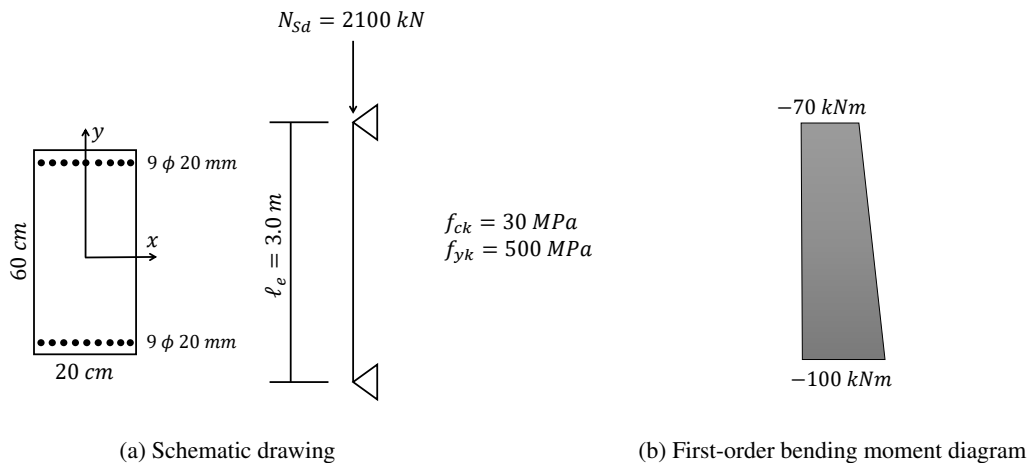


Figure 4. Case study initial data. Adapted from Casagrande [1].

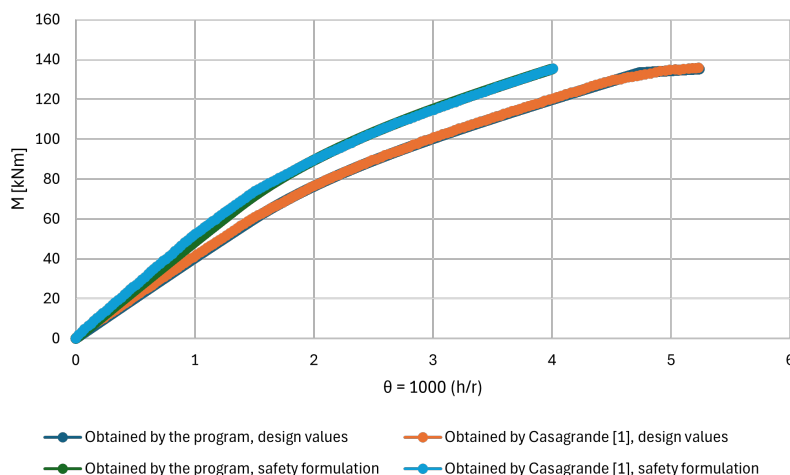


Figure 5. M, N,  $1/r$  diagram without creep.

From this diagram, the Standard-Column Method is applied, obtaining the maximum internal total moment in the column, resulting from the sum of first-order and second-order moments,  $M_{d,tot} = 118.84$  kN m. To this value, the moment resulting from the Approximate Method of Additional Eccentricity  $e_{cc}$ , with a creep coefficient  $\varphi = 2.0$ , is added, and final moment value obtained is  $M_d = 145.87$  kN m.

In the second strategy, the Standard-Column Method with creep incorporated is applied. In this method, the effective creep coefficient  $\varphi_{ef} = 1.18$  calculated according to Casagrande [1] is used. The M, N,  $1/r$  diagrams obtained are represented in Fig. 6. Similarly, the diagrams obtained for the design values and for the values obtained using the safety formulation in the developed program and in the work of Casagrande [1] are represented in the same figure. Analyzing the diagrams, a difference is observed in the final phase of the curves related to the values obtained with the safety formulation.

From this diagram, the Standard-Column Method is applied, obtaining the maximum internal total moment in the column with creep incorporated,  $M_{d,tot} = 132.21$  kN m. The result obtained by Casagrande [1] for the same method is  $M_{d,tot} = 130.40$  kN m.

By comparing the results of the two methods applied in this work, it is observed that the result obtained by the Approximate Method of Additional Eccentricity  $e_{cc}$  is approximately 12% higher, favoring safety.

Casagrande [1] analyzed the same column using more refined methods such as the General Method. In this method, the author obtained a result of  $M_{d,tot} = 129.41$  kN m, which is close to the result obtained in this work for the Standard-Column Method coupled with M, N,  $1/r$  diagram with incorporated creep.

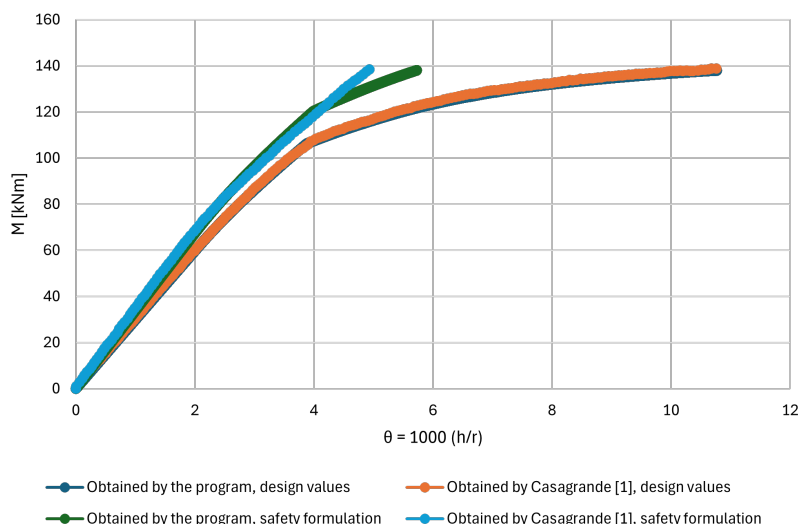


Figure 6.  $M, N, 1/r$  diagram with creep incorporated.

## 6 Conclusions

It is concluded that the Approximate Method of Additional Eccentricity  $e_{cc}$ , present in ABNT NBR 6118 [5], yields higher moment values. This safety-favorable approach is justified by its simplicity. On the other hand, the Standard-Column Method coupled with  $M, N, 1/r$  Diagrams with incorporated creep provides results close to more refined methods, still with relative ease of application.

Future steps of this study include the implementation of the General Methods and a Mathematical Model with analytical incorporation of the time variable for a more refined analysis of these columns, and the simulation of columns with different structural models.

**Acknowledgements.** The authors gratefully acknowledge the financial support provided by the Brazilian agencies FAPEMIG, CNPq and CAPES.

**Authorship statement.** The authors hereby confirm that they are the sole liable persons responsible for the authorship of this work, and that all material that has been herein included as part of the present paper is either the property (and authorship) of the authors, or has the permission of the owners to be included here.

## References

- [1] A. F. Casagrande. Consideração da fluência no cálculo dos efeitos de segunda ordem em pilares de concreto armado. Master's thesis, Universidade Federal de Santa Catarina, Florianópolis, SC, Brasil, 2016.
- [2] Y. Ballim and G. C. Fanourakis. Predicting creep deformation of concrete. *Proceedings, 11th FIG Symposium on Deformation Measurements*, vol. 1, 2003.
- [3] de L. A. F. Souza. Modelagem numérica computacional de viga de concreto armado com acoplamento de teorias. *Vetor*, vol. 22, n. 2, pp. 43–58, 2012.
- [4] R. C. Carvalho and L. M. Pinheiro. *Cálculo e detalhamento de estruturas usuais de concreto armado*, volume 2. Pini, São Paulo, 2009.
- [5] *ABNT NBR 6118*. Associação Brasileira De Normas Técnicas, Rio de Janeiro, 2023.
- [6] P. B. Fusco. *Estruturas de concreto - Solicitações normais*. Guanabara Dois S.A., 1981.
- [7] B. Westerberg. *Time-dependent effects in the analysis and design of slender concrete compression members*. PhD thesis, Instituto Real de Tecnologia, Estocolmo, 2008.
- [8] *Eurocode 2*. EUROPEAN COMMITTEE FOR STANDARDIZATION, 2004.
- [9] de J. A. Paula. Algoritmos para o estudo de pilares esbeltos de concreto armado solicitados a flexão normal composta. Master's thesis, Universidade de São Paulo, São Carlos, SP, Brasil, 1988.